The effect of neutral helper lipids on the structure of cationic lipid monolayers

A. P. Dabkowska[1], D. J. Barlow[1], A. V. Hughes[2], R. A. Campbell[3], P. J. Quinn[1] and M. J. Lawrence[1],*

[1]*Institute of Pharmaceutical Science, School of Biomedical Sciences, King's College London, 150 Stamford Street, London SE1 9NH, UK*
[2]*ISIS, Rutherford Appleton Laboratory, Chilton, Didcot OX11 0QX, UK*
[3]*Institut Laue-Langevin, B.P. 156, 38042 Grenoble Cedex, France*

Successful drug delivery via lipid-based systems has often been aided by the incorporation of 'helper lipids'. While these neutral lipids enhance the effectiveness of cationic lipid-based delivery formulations, many questions remain about the nature of their beneficial effects. The structure of monolayers of the cationic lipid dimethyldioctadecylammonium bromide (DODAB) alone, and mixed with a neutral helper lipid, either diolelyphosphatidylethanolamine or cholesterol at a 1 : 1 molar ratio was investigated at the air–water interface using a combination of surface pressure–area isotherms, Brewster angle microscopy (BAM) and specular neutron reflectivity in combination with contrast variation. BAM studies showed that while pure DODAB and DODAB with cholesterol monolayers showed fairly homogeneous surfaces, except in the regions of phase transition, monolayers of DODAB with diolelyphosphatidylethanolamine were, in contrast, inhomogeneous exhibiting irregular bean-shaped domains throughout. Neutron reflectivity data showed that while the thickness of the DODAB monolayer increased from 17 to 24 Å as it was compressed from a surface pressure of 5–40 mN m^{-1}, the thickness of the helper lipid-containing monolayers, over the same range of surface pressures, was relatively invariant at between 25 and 27 Å. In addition, the monolayers containing diolelyphosphatidylethanolamine were found to be more heavily hydrated than the monolayers of cationic lipid, alone or in combination with cholesterol, with hydration levels of 18 molecules of water per molecule of lipid being recorded for the diolelyphosphatidylethanolamine-containing monolayers at a surface pressure of 30 mN m^{-1} compared with only six and eight molecules of water per molecule of lipid for the pure DODAB monolayer and the cholesterol-containing DODAB monolayer, respectively.

Keywords: cationic lipid; neutral helper lipid; dioleylphosphatidylcholine; cholesterol; Brewster angle microscopy; specular neutron reflectivity

1. INTRODUCTION

Cationic lipid-based vehicles (known as lipoplexes) have long been used for the delivery of genetic material into cells [1]. However, it is widely recognized that the efficiency of nucleic acid delivery achieved using lipoplexes is limited, with the further problem that the cationic lipids employed are toxic to cells [2]. In an attempt to increase the transfection efficiency [3,4], at the same time mitigating the toxicity owing to the cationic lipids [5], neutral 'helper' lipids such as cholesterol and dioleoyl phosphoethanolamine (DOPE), are added to the lipid vesicles used in the preparation of DNA : lipid complexes, or lipoplexes.

One of the lipids used in the preparation of such lipoplexes (and the one chosen for this study) is the commercially available lipid, dimethyldioctadecylammonium bromide (DODAB). This lipid has been shown to be successful in delivering nucleic materials *in vitro* when used as sole lipid [6], although its effectiveness is increased in the presence of neutral helper lipids such as DOPE and the cholesterol derivative, PtdChol [7]. Previous studies have investigated the structure of a DODAB monolayer at the air–water interface [8–11], sometimes in the presence of DNA [12,13] but (to the authors' knowledge) there have been no studies concerned with the effect of a helper lipid on the structure of the DODAB lipid monolayer.

Based upon the findings of a number of small-angle X-ray scattering and optical microscopy studies, it has been proposed that the neutral helper DOPE aids transfection by promoting fusion of the vehicle with cellular membranes [14]. Cholesterol, in contrast, is

believed to improve transfection by protecting the DNA from degradation by DNases in the body [15] and may also have some effect on the fluidity of the cellular membrane [16]. In addition, cholesterol has been shown to be effective in reducing the binding of serum proteins to lipoplexes [17], thereby improving transfection of DNA, both *in vitro* and *in vivo*.

The aim of the present study was to lay the foundation for future studies on DODAB : DNA mixed monolayers by determining the effect of the neutral helper lipids on the conformation and packing of cationic lipid molecules used to prepare lipoplexes. Studies have shown that lipid monolayers at the air–water interface are good models of vesicles [18], which are used to prepare lipoplexes and have thus been used in the present study to investigate the changes elicited in the structure of cationic lipid monolayers by the presence of helper lipids. Neutron reflectivity and Brewster angle microscopy (BAM) studies of the lipid monolayers have been used here to determine the organization of the molecules comprising the monolayers across and parallel to the air–water interface, respectively. The effect on the structure of the DODAB monolayer was investigated for two of the most commonly used helper lipids—DOPE and cholesterol.

2. EXPERIMENTAL SECTION

2.1. Materials

Dimethyldioctadecylammonium bromide (MW 630.95 g mol^{-1}; >99.0% purity; $C_{38}H_{80}NBr$) was purchased from Sigma–Aldrich (Poole, Dorset, UK). Dimethyl-di(octadecyl-d$_{37}$)ammonium bromide (d$_{74}$-DODAB; MW 705.41 g mol^{-1}; 98% deuteration; $C_{38}H_6D_{74}NBr$) and di(methyl-d3)di(octadecyl)ammonium bromide (d$_3$-DODAB; MW 744.05 g mol^{-1}; 99% deuteration; $C_{38}H_{77}D_3NBr$) were purchased from CDN Isotopes (Quebec, Canada). Cholesterol (MW 386.66 g mol^{-1}; >98% purity; $C_{27}H_{45}OH$) and 1,2-dioleoyl-sn-glycero-3-phosphoethanolamine (DOPE; MW 744.05 g mol^{-1}; 100% purity; $C_{41}H_{78}NO_8P$) were obtained from Avanti Polar Lipids (Alabaster, AL, USA). In the case of d$_{74}$-DODAB, electrospray mass spectrometry (EPSRC National Mass Spectrometry Service Centre, Swansea) was also used to check purity. Ethanol (AnalaR) and chloroform (Spectroscopic grade) were purchased from BDH Chemical Ltd (Poole, Dorset, UK). Sodium chloride (NaCl; AnalaR, BDH Chemical Ltd) was heated to 530°C for 26 h in a muffle furnace in order to remove any organic contaminants. It was found that the NaCl, as provided by the manufacturer, lost less than 0.1 per cent of its mass during the dry combustion process. Water was either deionized water, double-distilled in a well-seasoned still (purity was regularly checked spectroscopically and by surface tensiometry—a surface tension of 72.8 ± 1 mN m^{-1} at 20°C was deemed acceptable), or purified using a Millipore Milli-Q system to a resistivity of 18 MΩ cm. D_2O (99.9% deuteration) was supplied by Aldrich.

2.2. Surface–pressure area (π–A) isotherms

Prior to all measurements, the Nima 601 Langmuir trough (Coventry, UK) was thoroughly cleaned, first with chloroform, then ethanol and finally copious amounts of ultrapure water. The trough was filled with 300 ml of an aqueous subphase containing 10 mM NaCl. Monolayers of DODAB or DODAB and helper lipid at a 1 : 1 molar ratio were prepared by depositing the lipids on the surface of the aqueous subphase from a chloroform solution (typically 20 μl of a approx. 2 mg ml^{-1} lipid solution) using a Hamilton syringe (Bonaduz, Switzerland). In the case of the mixed DODAB : helper lipid monolayers, the molecular weight used to calculate the area per molecule was the average of the molecular weights of the DODAB and the neutral helper lipid. The chloroform solvent was allowed to evaporate over approximately 10 min after which time the lipid film was compressed at a barrier speed of 30 cm^2 min^{-1} (corresponding to compression rates of 7.9 Å^2 per molecule-min for DODAB monolayers, 7.3 Å^2 per molecule-min for DODAB : cholesterol monolayers and 8.6 Å^2 per molecule-min for DODAB : DOPE monolayers), and the surface pressure (π)–area (A) isotherm was recorded. The surface pressure of the monolayer was continuously measured as a function of lipid molecular area using a Wilhelmy plate (10 × 50 mm filter paper; Whatman International, Maidstone, UK) immersed in the aqueous subphase and attached to a surface pressure sensor. Each experiment was repeated at least three times to ensure the reproducibility of the results. The stability of the lipid films was checked by maintaining the surface pressure at a predetermined value and monitoring any change in surface area over time. No change in the behaviour of the various DODAB-containing isotherms was observed over the temperature range used in this study, namely 22 ± 2°C.

2.3. Brewster angle microscopy

The surface of each lipid monolayer was imaged at predetermined surface pressures using a Brewster angle microscope (BAM2, NDF, Göttingen, Germany) mounted above a Nima 601 Langmuir trough (Coventry, UK) at 22 ± 2°C. The wavelength of the laser was 532 nm and the angle of incidence for all measurements was the Brewster angle for water (i.e. approx. 53° relative to the normal of the water surface). The BAM images were recorded on a charge-coupled device camera, such that the size represented by each image is 430 × 538 μm. The background was subtracted from each image; which was then corrected geometrically using image processing software (NDF). Each spread monolayer was compressed only once as the surface structure of the film was observed to vary slightly according to its history—as noted by previous workers [10]. However, repeated experiments were performed, each using a fresh monolayer to ensure that the images formed for a given system at a given surface pressure were reproducible.

2.4. Specular neutron reflectivity experiments

The specular neutron reflectivity (SNR) measurements of the DODAB-containing monolayers were carried out on the SURF beam line at the ISIS Facility, Rutherford Appleton Laboratory (Chilton, Oxfordshire, UK) and on the FIGARO beam line at the Institut

Table 1. Scattering lengths and molecular volumes used in this study.

material	molecular formula	molecular volume ($\mathring{A}^3$)	scattering length ($\times 10^4 \mathring{A}$)
$D_2O_{(s)}$	10 mM NaCl, D_2O	30	19.15
acmw$_{(s)}$	10 mM NaCl, H_2O/D_2O	30	0
DODAB	$C_{38}H_{80}N^+Br^-$	1174	-3.06
d$_{74}$-DODAB	$C_{38}D_{74}H_6N^+Br^-$	1174	72.66
cholesterol	$C_{27}H_{46}O$	630	1.32
DOPE	$C_{41}H_{78}NO_8P$	1230	4.16

Laue-Langevin (Grenoble, France). SURF data (figures 6–8 and electronic supplementary material, figures S3–S11) were collected at an incident angle (relative to the plane of the surface) of 1.5°; FIGARO data (figure 8 and electronic supplementary material, figures S9–S11) were collected at the incident angles of 0.62° and 3.8°. In both cases, instrument calibration was performed using a pure D_2O subphase. Flat backgrounds—the nature of which was confirmed visually for each dataset—were subtracted from all reflectivity profiles, with the background level for ISIS measurements determined by extrapolation to high momentum transfer, and for ILL measurements determined through the simultaneous acquisition of off-specular data on the area detector.

For each of the studied monolayer systems, the reflectivity measurements were recorded for three different (H/D) contrasts: d$_{74}$-DODAB on air-contrast matched water containing 10 mM NaCl (acmw$_{(s)}$; 10 mM NaCl in 0.92 H_2O: 0.08 D_2O), and either d$_{74}$-DODAB or protonated DODAB on a 10 mM NaCl D_2O subphase (denoted here as $D_2O_{(s)}$). The majority of the data were obtained using the SURF reflectometer at ISIS, although the data obtained for the mixed DODAB : DOPE monolayers were obtained through a combination of experiments performed at ISIS and at ILL. In the determination of partial structure factors for the DODAB : DOPE monolayers, therefore, because of differences in Q intervals for the SURF and FIGARO measurements, it was necessary to interpolate the FIGARO data points to give reflectivities at Q-values which matched those employed for SURF measurements. It should be noted here, however, that the resulting 'smoothing' of the FIGARO data in no way compromised either the resolution or the interpretation of the data, as the interpolations were only performed over very small intervals in Q, of the order of 0.005 $\mathring{A}^{-1}$.

The scattering lengths and volumes of the molecular components used in this study are summarized in table 1. The volume of the DODAB head group was calculated as the sum of the volumes of two methyl groups [19], a nitrogen and a bromide as calculated from the atomic radius, while the volume of the PE head group was the sum of the volumes of phosphate, glycerol, carbonyl and ethanolamine groups [19]. The volumes of the chains were calculated as the sum of CH_2, C = C and CH_3 groups as described by Armen *et al.* [19], while the volume of cholesterol was taken as reported from neutron diffraction and simulations of bilayers [20]. The scattering length was calculated from the atomic scattering length of the constituent atoms. The presence of 10 mM NaCl was determined to have a negligible effect on the scattering length density of the two sub-phases used. The DODAB-containing monolayers were prepared as described above using a NIMA trough (Coventry, UK) placed on an anti-vibration table. SNR measurements were performed on monolayers compressed (at a speed of 30 cm^2 min^{-1}) to the final maintained surface pressures of 5, 20, 30 and 40 mN m^{-1}. The monolayer reflectivities, $R(Q)$, were determined as a function of the momentum transfer, $Q = 4\pi\sin(\theta)/\lambda$, where θ and λ are, respectively, the angle of incidence (relative to the plane of the surface) and wavelength of the incident neutrons.

2.5. Neutron reflectivity data analysis

The neutron reflectivity data were modelled by means of simple Guinier(-type) analyses [21]—using the measurements made for deuterated systems only, to provide surfactant layer thicknesses and interfacial molecular areas—and by kinematic analyses [22,23]—using the measurements for all *h*- and *d*-contrasts, to provide surfactant layer thicknesses and molecular areas, and also the solvent layer thicknesses and surfactant–solvent separations.

For the monolayers involving d$_{74}$-DODAB spread on acmw containing 10 mM NaCl, the specular reflectivity ($R(Q)$) arises primarily from the interfacial layer and a (Guinier-type) plot of $\ln(R(Q).Q^2)$ versus Q^2 was used (via the slope, s) to provide an estimate of the second moment thickness of the distribution for the deuterated species, $\tau_A = \sqrt{(-s)}$, and (via the intercept on the ordinate, τ) to obtain an estimate of molecular area of the interfacial species, a_0, as:

$$\tau = \ln\left(16\pi^2 \frac{b_A}{a_0 N_A}\right), \qquad (2.1)$$

where N_A is Avogadro's number and b_A is the sum of the coherent scattering lengths.

Assuming then that the interfacial layer is modelled satisfactorily as a uniform slab, the thickness of the slab is obtained as $\tau_A\sqrt{12}$, and if we assume instead a Gaussian distribution of width σ_A, we have $\sigma_A = \tau_A\sqrt{8}$.

Following the kinematic approximation, the SNR profiles were also analysed in terms of partial structure factors for the molecular components of the monolayers [24]. The components considered included the solvent within the monolayer and either the DODAB molecule (for the DODAB monolayer) or the DODAB : helper lipid 'super-molecule' (for the DODAB : cholesterol or DODAB : DOPE monolayers). The term 'super-molecule' is used to describe the combined areas of the DODAB and

the helper lipid molecules. In the latter case, it should be noted that the device of the super-molecule (with DODAB and the helper lipid being treated as a single entity) was used purely as an analytical convenience, dictated by the fact that the helper lipids were used only in their undeuterated form, and does not imply any specific complexation between DODAB and the helper lipid. (In order, therefore, to compare the interfacial areas obtained from SNR with those obtained from the Langmuir isotherm studies, it is necessary to divide the former by a factor of two.) The three partial structure factors, h_{AA}, h_{SS}, and h_{AS} were determined and describe the distributions of the lipid/amphiphile (A) and the solvent (S), and the cross-term between these two distributions. The monolayer reflectivity can be defined as:

$$R(Q) = 16\frac{\pi^2}{q^2}\left(b_A^2 h_{AA}(Q) + b_S^2 h_{SS}(Q) + 2b_S b_A h_{SA}(Q)\right), \quad (2.2)$$

where Q is the momentum transfer and b_A and b_S are the sums of the atomic scattering lengths (in ångströms) for the lipid and the solvent, respectively.

The partial structure factor for the lipid distribution, $h_{AA}(Q)$ was modelled using a Gaussian function:

$$h_{AA}(Q) = \pi\sigma_A n_{A0}^2 \exp\left(\frac{-q^2\sigma_A^2}{8}\right), \quad (2.3)$$

where n_{A0} is the surface excess and σ_A is the Gaussian width of the distribution. The distribution of the solvent across the interface was modelled assuming a tanh profile, thus the solvent structure factor, h_{SS}, is then given as:

$$h_{SS}(Q) = n_0^2\left(\xi\frac{\pi}{2}\right)^2 \operatorname{cosech}^2\left(\xi\pi\frac{q}{2}\right), \quad (2.4)$$

where ζ is the width of the layer and n_0 is the bulk solution number density, constrained as $0.0333\ \text{Å}^{-3}$. The partial structure factor h_{SA} describing the cross term for the lipid and the solvent distributions was modelled as:

$$h_{SA}(Q) = (h_{SS}h_{AA})^{1/2}\sin(q\delta_{SA}), \quad (2.5)$$

where δ_{SA} is the separation between the midpoints of the two distributions.

3. RESULTS AND DISCUSSION

3.1. Surface–pressure area (π–A) isotherms

The effect of the helper lipids, cholesterol and DOPE, on DODAB monolayers was studied by determining their π–A isotherm when spread on an aqueous subphase containing 10 mM NaCl. The isotherm for DODAB on the 10 mM NaCl aqueous subphase (solid line, figure 1) exhibits an expanded region at large areas per molecule, with a plateau at intermediate areas per DODAB molecule of between 90 and 65 Å^2, and a condensed region at areas per molecule of less than 62 Å^2. Contrary to other researchers who report a large hysteresis for DODAB monolayers on pure water [10], we here observed only a very slight hysteresis upon decompression and recompression of the DODAB film (electronic supplementary
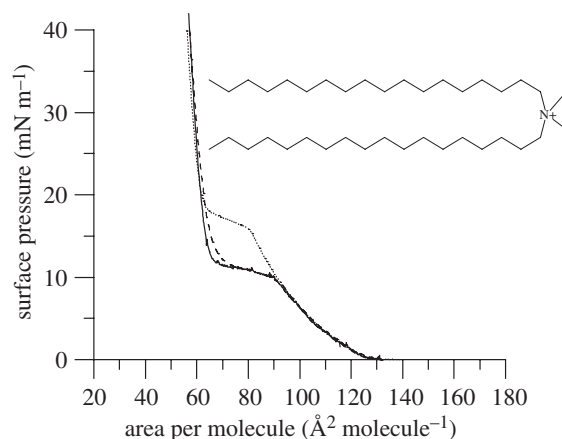

Figure 1. Surface pressure–area isotherms of DODAB on 10 mM NaCl subphase. Protonated DODAB (solid line), d$_3$-DODAB (dashed line) and d$_{37}$-DODAB (dotted line) at 22°C, Number of repeats $n = 3$. The molecular structure of DODAB (inset).

material, figure S1). To err on the side of caution, however, each DODAB-containing monolayer examined in the present study was freshly prepared. Electronic supplementary material, figure S2 gives an example of an isotherm showing the collapse of a DODAB monolayer on an aqueous subphase containing 10 mM NaCl. As previously noted by Vranken *et al.* [9], published isotherms of DODAB vary in terms of collapse surface pressure, lift-off area, and position and length of the plateau, owing to the sensitivity of the lipid to temperature and subphase salt concentration, and the isotherm reported here, although qualitatively similar, differs in terms of the aforementioned features from those presented for DODAB on pure water (see [8,9,11,25–28]).

Isotherms of the monolayers formed by the head group (d$_3$-) and chain (d$_{74}$-) deuterated versions of DODAB were also examined (figure 1) in order to verify that deuteration of the DODAB molecule did not cause any significant deviation in surface behaviour, particularly at the surface pressures of interest here, namely 5, 20, 30 and 40 mN m^{-1}. Although not used in the present study, the d$_3$-DODAB (dashed line, figure 1) exhibited an isotherm very similar to that of DODAB—the slightly larger area per molecule seen in the first part of the condensed region being a consequence of the low level of deuteration present in the head group. In contrast, however, the isotherm of the alkyl chain (d$_{74}$-) deuterated version of DODAB (dotted line, figure 1) was significantly different from that of DODAB but only in the region of the phase transition of the lipid monolayer from its expanded to its condensed phase, as in other regions, the isotherms overlay one another. In particular, the phase transition of the d$_{74}$-DODAB film occurs at a smaller area per molecule than for the hydrogenous form. This result was not unexpected because it is well-known that chain deuteration affects the phase transition of lipids in that the chain-deuterated form of the lipid exhibits a slight reduction in the temperature of the onset of the change from a gel to liquid crystalline phase
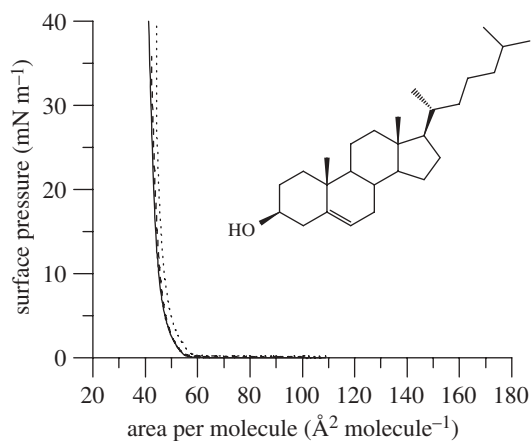
Figure 2. Surface pressure–area isotherms of DODAB : cholesterol (1 : 1 molar mixture) on 10 mM NaCl subphase. Protonated DODAB : cholesterol (solid line), d$_3$-DODAB : cholesterol (dashed line) and d$_{37}$-DODAB : cholesterol (dotted line) at 22°C, $n = 3$. The molecular structure of cholesterol (inset).
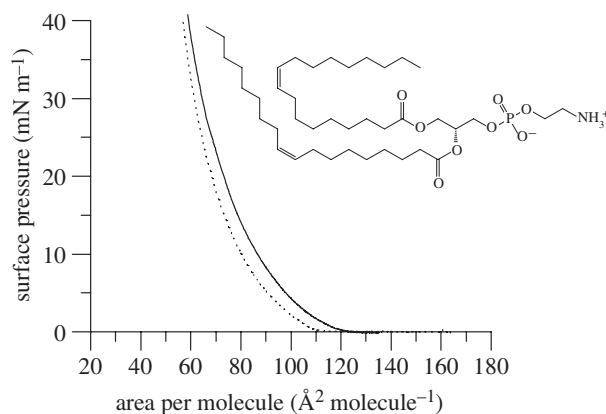

Figure 3. Surface pressure–area isotherms of DODAB : DOPE (1 : 1 molar mixture) on 10 mM NaCl subphase. Protonated DODAB : DOPE (solid line), d$_3$-DODAB : DOPE (dashed line) and d$_{37}$-DODAB : DOPE (dotted line) at 22°C, $n = 3$. The molecular structure of DOPE (inset).

[29,30]. This effect is thought to be owing to the slightly lower value of the CD bond length compared with that of the CH bond resulting in a decrease in the interlocking of the hydrocarbon chains which facilitates the onset of disorder at lower temperatures. Fortunately for the present study, the effect of chain-deuteration is not noticeable at the surface pressures employed in the subsequent BAM and neutron reflectivity studies.

The isotherm of a unimolar mixture of DODAB : cholesterol on an aqueous subphase containing 10 mM NaCl (figure 2) was different from that obtained using pure DODAB in that it exhibited no discernable phase transition, almost immediately forming a condensed phase at average areas per molecule smaller than approximately 55 Å^2. It is clear that the presence of cholesterol abolishes the abrupt phase transition from expanded to condensed phase observed for pure DODAB monolayers. Furthermore, the collapse surface pressure increased from approximately 50 mN m^{-1} observed for the pure DODAB monolayer to approximately 55 mN m^{-1} (electronic supplementary material, figure S2) indicating the production of a more stable film. No hysteresis for the DODAB : cholesterol monolayer was noticed upon repeated compression and decompression of the monolayer film.

The addition of the sterol to the DODAB monolayer caused a shift in the isotherm (figure 2) towards a smaller average molecular area (i.e. approx. 42 Å^2 per molecule at 40 mN m^{-1}) than would be expected from a consideration of the isotherms observed for DODAB (i.e. 57 Å^2 per molecule at 40 mN m^{-1}) and cholesterol alone (i.e. approx. 38 Å^2 per molecule at 40 mN m^{-1}) assuming ideal mixing. It is well-known that cholesterol exhibits a considerable condensing effect when mixed with other lipids (cf. [31]) and molecular dynamics simulations have shown that the effective cross-sectional area of cholesterol, when in combination with saturated phospholipids, can be approximately 33 Å^2 [32] or even as low as approximately 22 Å^2 [33]—a much smaller value than the limiting area of 39 Å^2 observed upon compression of a pure cholesterol

monolayer [27,34]. Reassuringly, the isotherm measured for DODAB/cholesterol in the present study is similar to that reported for the same lipid mixture by Hac-Wydro *et al.* [27]. Electronic supplementary material, figure S1 shows that there was no hysteresis observed for the mixed DODAB : cholesterol monolayer (also consistent with the findings of Hac-Wydro *et al.*) and only a slight difference in the isotherm obtained for the mixed d$_{74}$-DODAB : cholesterol monolayer (figure 2, dotted line).

In contrast to the DODAB monolayers containing cholesterol, the isotherm of an equimolar mixture of DODAB : DOPE on an aqueous subphase of 10 mM NaCl (figure 3) exhibited and remained in an expanded state from the lift-off area of approximately 120 Å^2 until its collapse at an area per molecule of approximately 60 Å^2. As was the case for the cholesterol-containing monolayer, the presence of DOPE as helper lipid abolished the phase transition observed for the monolayer comprising only DODAB. Like the DODAB and DODAB : cholesterol monolayers, the DODAB : DOPE monolayer showed little hysteresis upon recompression (electronic supplementary material, figure S1). Electronic supplementary material, figure S2 gives an example of an isotherm showing the collapse of a DODAB monolayer on an aqueous subphase containing 10 mM NaCl, and shows that the addition of DOPE to the DODAB monolayer produces a slightly more stable film.

3.2. Brewster angle microscopy

BAM images were collected at several points during the compression of DODAB, DODAB : cholesterol and DODAB : DOPE monolayers on an aqueous subphase containing 10 mM NaCl (figure 4). The pure DODAB monolayer appeared homogeneous in the expanded region of the isotherm, i.e. less than 5 mN m^{-1} while in the plateau region, very small circular domains were initially observed, these structures then changing into large flower-like domains (of diameter 30–50 μm) upon further compression, eventually fusing to form a more homogeneous film containing a very small number of
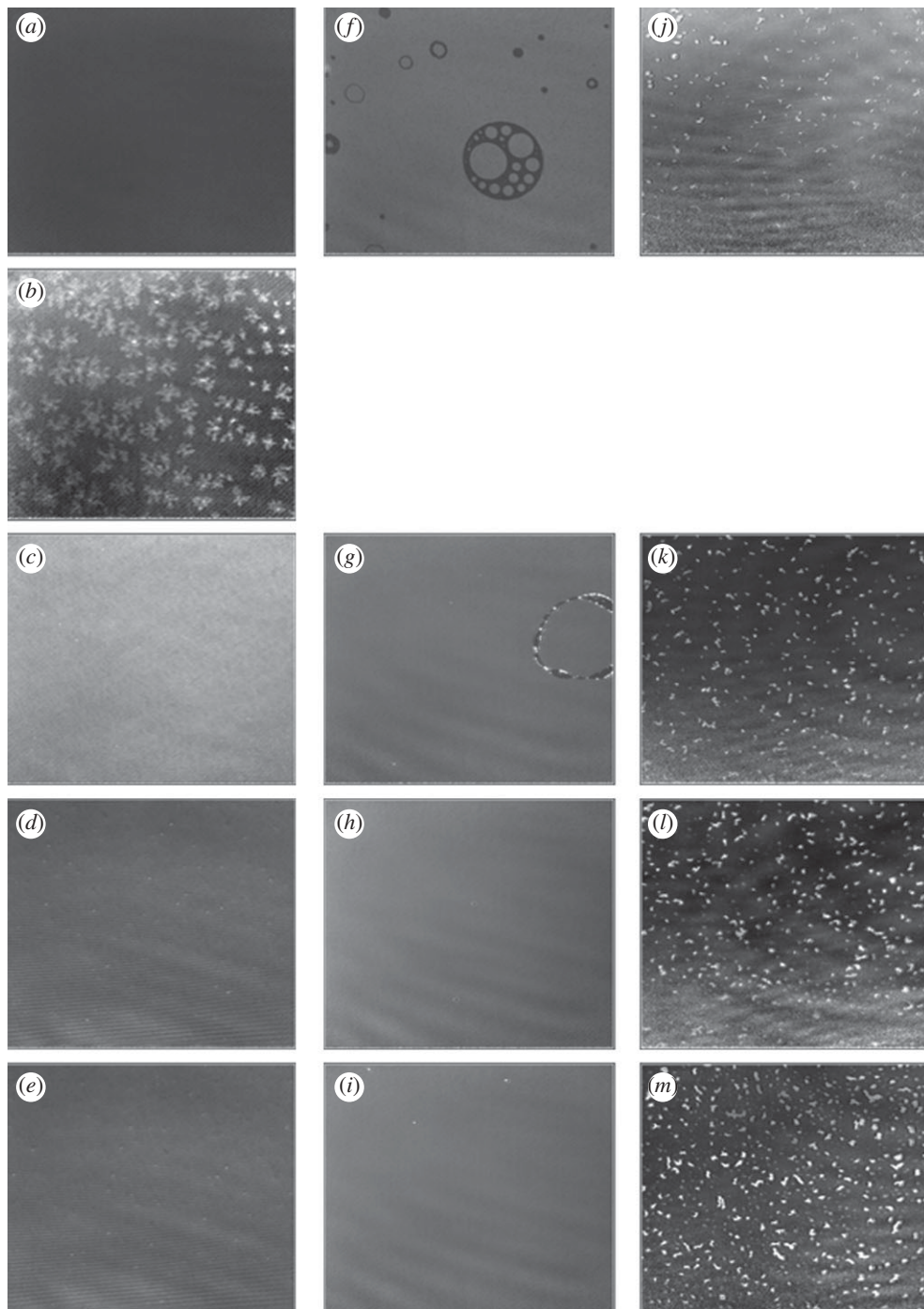
Figure 4. BAM images of monolayer on a 10 mM NaCl subphase: DODAB compressed to (*a*) $5 \, \text{mN m}^{-1}$, (*b*) $13.4 \, \text{mN m}^{-1}$, (*c*) $20 \, \text{mN m}^{-1}$, (*d*) $30 \, \text{mN m}^{-1}$ and (*e*) $40 \, \text{mN m}^{-1}$; DODAB : cholesterol compressed to (*f*) $5 \, \text{mN m}^{-1}$, (*g*) $20 \, \text{mN m}^{-1}$, (*h*) $30 \, \text{mN m}^{-1}$ and (*i*) $40 \, \text{mN m}^{-1}$; DODAB : DOPE compressed to (*j*) $5 \, \text{mN m}^{-1}$, (*k*) $20 \, \text{mN m}^{-1}$, (*l*) $30 \, \text{mN m}^{-1}$ and (*m*) $40 \, \text{mN m}^{-1}$. The size represented by each image is $430 \times 538 \, \mu\text{m}$.

small, circular domains in the surface pressure range $20–40 \, \text{mN m}^{-1}$. These results are very similar to those of DODAB monolayers reported by Sun *et al.* [12], although the lift-off area and location of the plateau occur at slightly different points on the isotherm owing to the differing experimental conditions.

The mixed DODAB : cholesterol monolayer appeared homogeneous when visualized by BAM. However, at very low surface pressures (less than or equal to $5 \, \text{mN m}^{-1}$), the BAM images typically revealed the presence of 'bubble-like' features, which disappeared

upon further compression—these structures are consistent with those previously reported for pure cholesterol monolayers [35]. Sparse domains were also present at higher surface pressures but these domains became smaller and scarcer as the surface pressure was increased beyond $30 \, \text{mN m}^{-1}$ when the monolayer appeared to be homogeneous.

BAM images of the mixed DODAB : DOPE monolayer revealed the presence of small, irregular bean-shaped domains that became more densely packed upon compression, although at surface pressures

of up to 40 mN m^{-1}, the domains did not fuse to form a film of homogeneous thickness. As this mixed monolayer does not undergo a phase transition (as evident in the recorded π–A isotherm), it is not unexpected that the domains remain during compression.

The chemical composition of these domains is not known but their presence signifies that, at the compositions used in the present study, the DODAB : DOPE monolayers are not ideally miscible. The heterogeneity of the monolayer will probably result in regions of the monolayer having different properties, such as charge density and lipid ordering, which may have implications for the binding of DNA. Significantly, however, from the point of view of the SNR measurements, the sizes of the individual domains and their clusters ($\sim 8\,\mu$m and $<20\,\mu$m, respectively) were smaller than the coherence length of the neutrons ($20-40\,\mu$m for the slit geometries used in the present SNR study). Consequently, any diffuse scattering arising from these phase-separated domains would not be expected to contribute significantly to the measured specular reflection. Therefore, the results of the analysis of the SNR data can be reasonably assumed to represent an average for the monolayer.

3.3. Specular neutron reflectivity

The SNR profiles measured for DODAB, DODAB : cholesterol and DODAB : DOPE monolayers on the 10 mM NaCl-containing aqueous subphase at 5, 20, 30 and 40 mN m^{-1} were analysed by means of Guinier plots (figure 5 and table 2) and in terms of partial structure factors and sample data for the latter are shown for all three DODAB-containing monolayers in figures 6–8. Note that data collected at surface pressures other than 40 mN m^{-1} are presented in the electronic supplementary material. The structural parameters derived through these analyses were in all cases broadly consistent with the corresponding estimates derived from the Guinier plots (figure 5). It should be noted, however, that in the Guinier analyses, only the SNR data for the chain-deuterated DODAB molecule on acmw$_{(s)}$ were used, which means that the derived monolayer thickness values only really provide estimates of the C18 hydrophobe thickness and they are thus somewhat smaller than the values obtained from the corresponding partial structure factor analyses (which estimates the distribution width for the whole molecule).

The lipid distribution (h_{AA}) partial structure factor revealed that the monolayer of pure DODAB (figure 6 and electronic supplementary material, figures S3–S5) increased in slab thickness, t_A, upon compression (table 3). At a surface pressure of 5 mN m^{-1}, the monolayer was relatively disordered with t_A of 16.8 Å but upon compression to 20 mN m^{-1} became more ordered with t_A of 22.4 Å. There was however only a small increase in thickness upon further compression of the monolayer to 40 mN m^{-1}, reflecting the steeper nature of the isotherm in this region (figure 1). Ellipsometric studies have previously shown that the Gaussian thickness (i.e. the width of the lipid distribution, σ) of a monolayer of DODAB deposited on pure water at a surface pressure of 35 mN m^{-1} and area per molecule of
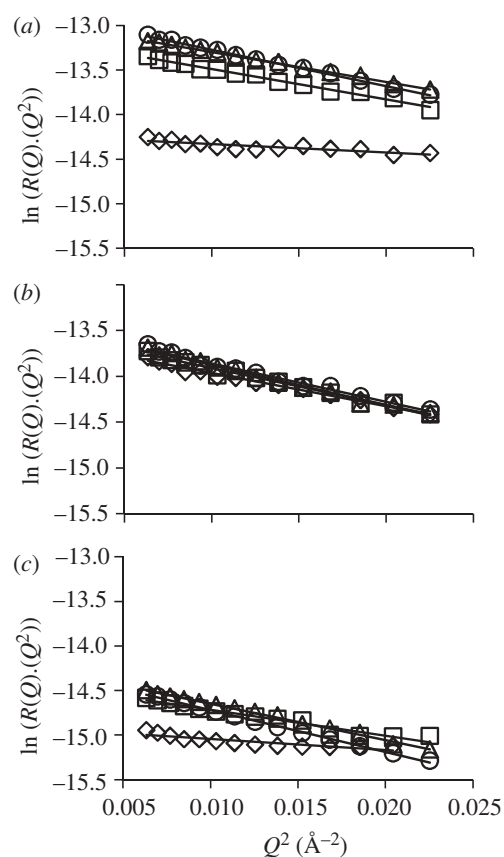

Figure 5. Guinier-type transformations derived from SNR profiles recorded for monolayers of (a) d$_{74}$-DODAB, (b) d$_{74}$-DODAB:cholesterol and (c) d$_{74}$-DODAB : DOPE on a subphase of acmw$_{(s)}$ at surface pressures of 5 mN m^{-1} (open diamonds), 20 mN m^{-1} (open squares), 30 mN m^{-1} (open triangles) and 40 mN m^{-1} (open circles). Black lines show the fits to the data in the domain where, as required [21], Qz is small.

58 Å^2, is around 21 Å [36]. The difference between this value and the slightly larger values reported here (22.9 and 24.0 Å at 30 and 40 mN m^{-1}, respectively; table 3), may be a consequence of the assumptions made in the calculation of the refractive index used for fitting the ellipsometric data [36].

Although a similar trend in monolayer slab thickness, t_A, was observed from the Guinier type analysis in that t_A increased with increasing surface pressure from 15.9 Å at 5 mN m^{-1} to 22.5 Å at 40 mN m^{-1} (table 2), the thicknesses of the monolayer obtained were up to 8 per cent lower than that obtained from the partial structure factor analysis (table 3) and is a consequence of the fact that the Guinier type analysis is derived using just one contrast, namely d$_{74}$-DODAB monolayers on acmw$_{(s)}$. Regardless of the origin of these small differences, however, both analyses indicate that at the lower surface pressures, the DODAB molecules are either disordered and/or tilted, as the length of the fully extended (all *trans*) alkyl chain is calculated as 23.0 Å. The length of the entire DODAB molecule is thus calculated to be approximately 27 Å, i.e. the length of the fully extended chain plus the length of the head group (here taken as approx. 4 Å, using the experimental result obtained
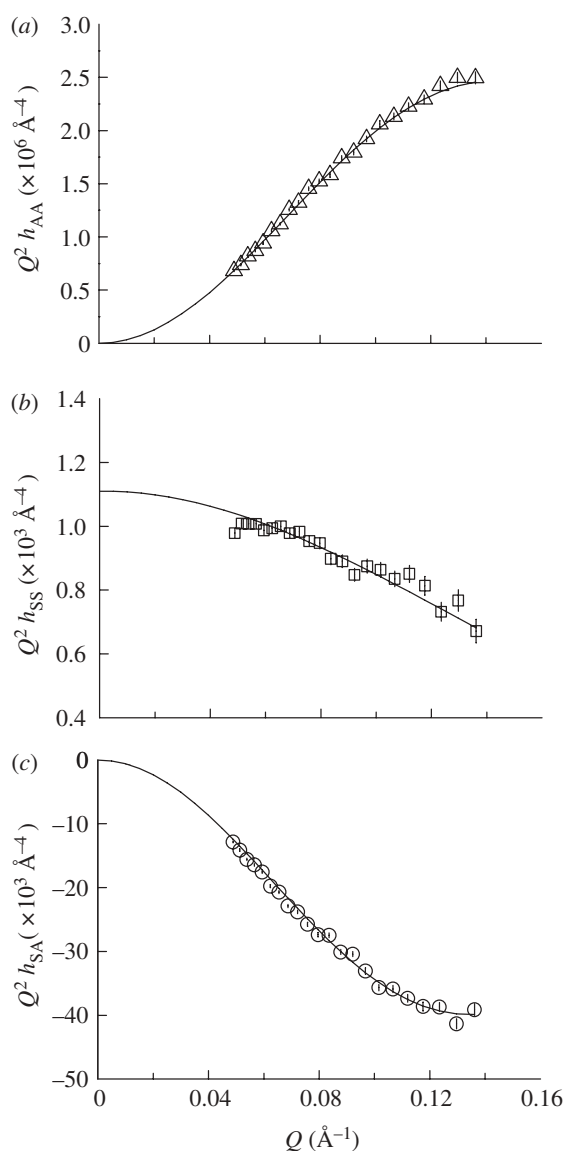
Figure 6. Plots of partial structural factors (*a*) $h_{AA}(Q)$ versus Q, (*b*) $h_{SS}(Q)$ versus Q and (*c*) $h_{SA}(Q)$ versus Q for DODAB monolayers at the surface pressure of 40 mN m^{-1}.

Figure 7. Plots of partial structural factors (*a*) $h_{AA}(Q)$ versus Q, (*b*) $h_{SS}(Q)$ versus Q and (*c*) $h_{SA}(Q)$ versus Q for DODAB : cholesterol monolayers at 40 mN m^{-1}.

by others [37] for the same head group in dihexa-decyldimethylammonium bromide). Using a thickness of 27 Å, the tilt angle is calculated to be 27° at 40 mN m^{-1}, which indicates that the DODAB molecules are slightly more upright than the measured tilt angle of 35° reported by others at 35 mN m^{-1} [36].

The areas per molecule obtained from the Guinier plots were consistent with those obtained by partial structure factor analysis, as well as those extrapolated from the surface pressure–area isotherm (electronic supplementary material, table S1). As expected, for the DODAB monolayers, the thicknesses obtained (table 3) suggest that at low surface pressures, i.e. less than 10 mN m^{-1}, the lipid chains are relatively disordered and/or tilted but that this disorder decreases as the monolayer is compressed.

The solvent separation (δ_{SA}), obtained from equation (2.5), and the partial structure factor (h_{SA}) describing the cross term for the lipid and the solvent distributions showed the distance between the
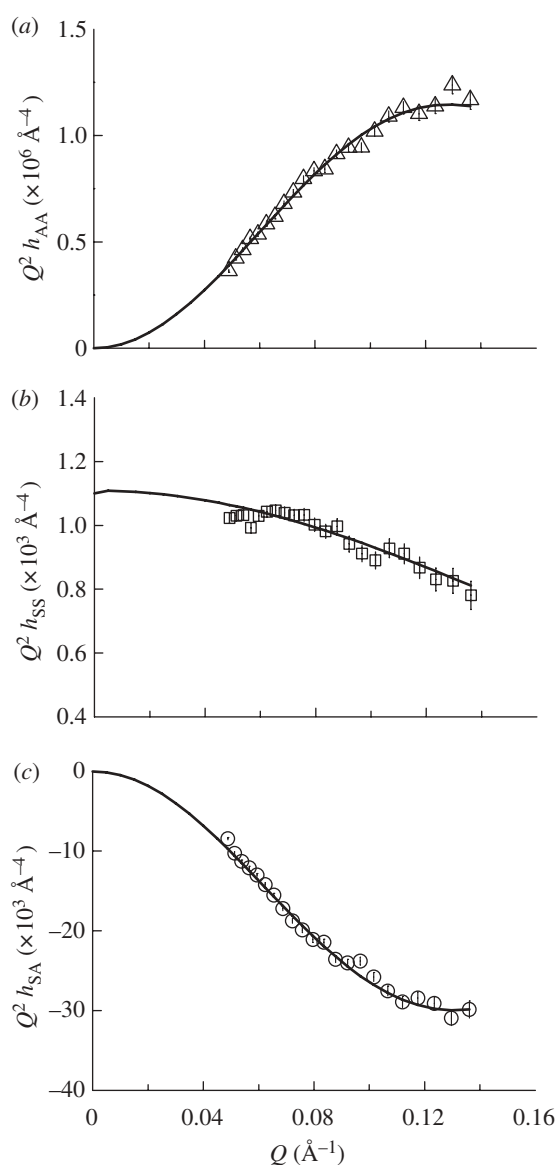
midpoint of the DODAB distribution and the midpoint of the solvent distribution to be 5.9 Å at a surface pressure of 5 mN m^{-1} (table 3), and suggest that the solvent partially wets the DODAB molecule when DODAB is in its expanded phase. As the monolayer was compressed to 20 mN m^{-1} (electronic supplementary material, figure S4) where the DODAB monolayer is in its condensed form (figure 1), the solvent separation rapidly increased to 9 Å and thereafter hardly changed upon the further compression of the monolayer to 40 mN m^{-1} (table 3). The increase in solvent separation between surface pressures of 5 and 20 mN m^{-1} (table 3) is attributed to a decrease in the tilt on the DODAB chains and head groups. In addition, the thickness of the solvent layer was 4–6 Å (table 3) suggesting that when DODAB is in its condensed state, only the head group region of the DODAB layer is wetted, as the thickness of the solvent layer is consistent with the thickness of the head group region (at approx. 4 Å).
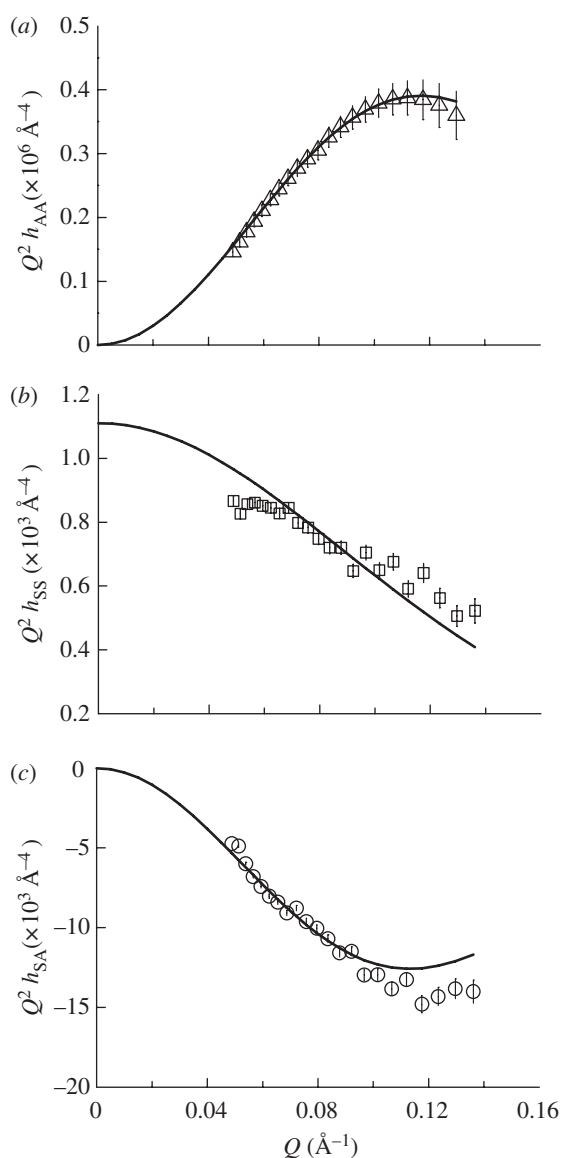
Figure 8. Plots of partial structural factors (*a*) $h_{AA}(Q)$ versus Q, (*b*) $h_{SS}(Q)$ versus Q and (*c*) $h_{SA}(Q)$ versus Q for DODAB : DOPE monolayers 40 mN m^{-1}.

The thickness of the pure DODAB monolayer at a surface pressure of between 30 and 40 mN m^{-1} (the lateral surface pressure in a cellular membrane is generally considered to be 30–35 mN m^{-1} (reviewed in [38–40])) when expressed as the thickness of the equivalent slab was between 22 and 24 Å (table 3). This value was satisfyingly close to half the thickness of the DODAB bilayer calculated to be 44.0 ± 1 Å on the basis of small-angle neutron scattering studies on unilamellar vesicles of diameter 80 ± 34 nm [41], and suggests that the DODAB bilayer does not exhibit any interdigitation, showing that the parameters obtained for the DODAB monolayer are a good model for 'one half' of the bilayer.

In order to determine the hydration of the lipids as described by Ma *et al.* [42], the number densities of the components of the monolayer were calculated in the *z*-direction (data not shown). At each point in the *z*-direction, z_i, the quotient of the number densities, n, of the two components, $n_S(z_i)/n_L(z_i)$, where n_S and n_L

are the number of solvent and lipid molecules, respectively, gives the number of water molecules associated with the DODAB molecule at that position in the monolayer. Here, the ratio was calculated at the midpoint of the DODAB distribution (z_m), with the integration performed between the limits $z_m \pm x$, where x is half of the thickness of the DODAB molecule determined at the relevant surface pressure. (For example, $x = 12$ Å in the case of the DODAB molecule at a surface pressure of 40 mN m^{-1}; table 3.) This approach thus gives the number of water molecules associated with each DODAB molecule (table 3). The DODAB monolayer is most heavily hydrated at 5 mN m^{-1} where there are 19 water (H$_2$O) molecules found for each DODAB molecule. This value decreased dramatically as the monolayer was compressed, and after the plateau region, the hydration of the DODAB monolayer was found to be approximately seven H$_2$O molecules per lipid. This is slightly higher than the figure of five H$_2$O molecules obtained for a phosphocholine head group from SNR studies [43], which is unexpected because evidence from gravimetric water adsorption studies suggests that while the choline component is responsible for strong water binding of lipids, a phosphatidylcholine head group adsorbs more water than a choline moiety [44].

The partial structure factor analysis revealed that the addition of the neutral helper lipid, cholesterol, significantly altered the structure of the DODAB-containing monolayer (figure 7, table 4 and electronic supplementary material figures S6–S8). Initially, the slab thickness of the DODAB-containing monolayer at 5 mN m^{-1} was increased from 17 Å in the absence of cholesterol (table 3) to 26 Å in its presence (table 4). Thereafter, the thickness of the monolayer increased steadily to 27 Å at 40 mN m^{-1} (and the Guinier analysis showed a similar trend, table 2). This monolayer thickness is more akin to the calculated thickness of a fully extended DODAB molecule than the value obtained from the DODAB monolayer as would be expected from the well-known condensing effect of cholesterol [34], which was observed at all surface pressures investigated in the present study.

The area of the DODAB : cholesterol super-molecule was found to decrease from 81 to 73 Å^2 upon increasing the surface pressure from 5 to 40 mN m^{-1} (table 4). The value of the area per super-molecule is slightly lower than twice the limiting average area per molecule of 42 Å^2 obtained from extrapolation of the isotherm (electronic supplementary material, table S1). Given the well-known errors inherent in determining the area per molecule from Langmuir isotherms [45], it is thought that these differences are not significant. More importantly, the small change in thickness and area per super-molecule with surface pressure (table 4) is consistent with the surface pressure–area isotherm measured, which showed that the mixed DODAB : cholesterol monolayer is in a condensed phase even at very low surface pressures (figure 2).

As the hydrophobic chains in the DODAB : cholesterol monolayer are expected to adopt a more upright position than those in the pure DODAB monolayer, it is not surprising that the solvent separation is also greater than

Table 2. Structural parameters for deuterated lipid monolayers on 10 mM NaCl acmw$_{(s)}$ subphase at various surface pressures, derived from the Guinier-type transformation of reflectivity profiles. The Guinier area per molecule or super-molecule in the case of the lipid mixtures (a_0) and the slab thickness of the layer (t_A) were derived from the intercept and the slope of the plots shown in figure 5, respectively. Note that for the monolayers containing helper lipids, the reported area is a sum of the areas of DODAB with cholesterol or DODAB with DOPE. The error is that calculated in the regression analysis.

lipid		$5 \, \mathrm{mN \, m^{-1}}$	$20 \, \mathrm{mN \, m^{-1}}$	$30 \, \mathrm{mN \, m^{-1}}$	$40 \, \mathrm{mN \, m^{-1}}$
d$_{74}$-DODAB	a_0 (Å^2)	107 ± 1	65 ± 1	60 ± 1	56 ± 1
	t_A (Å)	15.9 ± 0.6	20.7 ± 0.1	20.9 ± 0.2	22.5 ± 0.4
d$_{74}$-DODAB : cholesterol	a_0 (Å^2)	82 ± 1	79 ± 1	78 ± 1	77 ± 1
	t_A (Å)	20.7 ± 0.3	21.2 ± 0.3	20.3 ± 0.4	21.8 ± 0.4
d$_{74}$-DODAB : DOPE	a_0 (Å^2)	155 ± 1	124 ± 1	119 ± 1	119 ± 1
	t_A (Å)	18.2 ± 0.6	20.3 ± 0.2	20.4 ± 0.4	24.1 ± 0.2

Table 3. Structural parameters for DODAB monolayer on a subphase containing 10 mM NaCl (obtained from partial structure factors). a_0 is the area per DODAB molecule; σ_A is the width of the lipid (Gaussian) distribution; t_A is the slab thickness where $t_A = \sigma_A \times (\sqrt{12}/\sqrt{8})$; δ_{SA} is the solvent separation, i.e. the distance from midpoint of lipid to midpoint of solvent distributions; ζ_S is the width of the solvent distribution; H is the number of water molecules associated with each lipid as calculated from the number density profiles of the water and lipid. The quoted error is the estimated error.

	$5 \, \mathrm{mN \, m^{-1}}$	$20 \, \mathrm{mN \, m^{-1}}$	$30 \, \mathrm{mN \, m^{-1}}$	$40 \, \mathrm{mN \, m^{-1}}$
a_0 (Å^2)	108 ± 1	64 ± 1	58 ± 1	56 ± 1
σ_A (Å)	14 ± 1	18 ± 1	19 ± 1	20 ± 1
t_A (Å)	17 ± 1	22 ± 1	23 ± 1	24 ± 1
δ_{SA} (Å)	6 ± 1	9 ± 1	10 ± 1	10 ± 1
ζ_S (Å)	4 ± 1	5 ± 1	5 ± 1	6 ± 1
H (H$_2$O/lipid)	19	7	6	7

Table 4. Structural parameters for 1 : 1 DODAB : cholesterol monolayers on a subphase containing 10 mM NaCl (obtained from partial structure factors). Symbols used as defined in table 3. a_0 is the area per molecule of the DODAB : cholesterol super-molecule. The quoted error is the estimated error.

	$5 \, \mathrm{mN \, m^{-1}}$	$20 \, \mathrm{mN \, m^{-1}}$	$30 \, \mathrm{mN \, m^{-1}}$	$40 \, \mathrm{mN \, m^{-1}}$
a_0 (Å^2)	81 ± 1	77 ± 1	74 ± 1	73 ± 1
σ_A (Å)	21 ± 1	21 ± 1	22 ± 1	22 ± 1
t_A (Å)	26 ± 1	26 ± 1	27 ± 1	27 ± 1
δ_{SA} (Å)	9 ± 1	9 ± 1	10 ± 1	10 ± 1
ζ_S (Å)	4 ± 1	4 ± 1	4 ± 1	5 ± 1
H (H$_2$O/lipid)	8	8	8	8

that seen for the DODAB monolayer. In addition, the solvent separation in the DODAB : cholesterol monolayer is only slightly increased from approximately 9 to 10 Å upon increasing the surface pressure from 5 to 40 mN m^{-1} (table 4). In contrast to the pure DODAB monolayer (table 3), there was no discontinuity in either the thickness of the cholesterol-containing monolayer or the solvent separation as the monolayer did not undergo a phase transition.

The steep isotherm (figure 2) and small decrease in the area per super-molecule upon compression derived from the SNR data (table 4) are owing to the ordering effect of the cholesterol, which probably causes the alkyl chains of DODAB to adopt a more vertical orientation in the monolayer, as derived from the increased thickness, even at low surface pressures. It should be noted that analysis of the SNR data yields an average thickness for the mixed monolayer. Furthermore, as the

length of a cholesterol molecule is reported to be approximately 17 Å [46], it is reasonable to assume that the slab thickness (t_A) of 26–27 Å determined for DODAB : cholesterol mixed monolayer is a consequence of the DODAB chains being oriented vertically at the air–water interface, even at low surface pressures. This conclusion is further supported by a hydration value of approximately eight H$_2$O/super-molecule obtained in the present study, which was found to be relatively invariant with surface pressures (table 4). Cholesterol has been shown (using a combination of neutron diffraction and simulation) to be hydrated by only one H$_2$O per cholesterol molecule [20].

In contrast to the cholesterol-containing DODAB monolayer, the DOPE-containing monolayer, was in the expanded phase, and the SNR studies showed that the slab thickness of the monolayer increased steadily as the monolayer was compressed, from 25 Å at

Table 5. Structural parameters for 1 : 1 DODAB : DOPE monolayers on a subphase containing 10 mM NaCl (obtained from partial structure factors). Symbols used as defined in table 3. a_0 is the area per moleule of the DODAB : DOPE super-molecule. The quoted error is the estimated error.

	5 mN m^{-1}	20 mN m^{-1}	30 mN m^{-1}	40 mN m^{-1}
a_0 (Å^2)	158 ± 1	124 ± 2	117 ± 1	116 ± 1
σ_A (Å)	19 ± 1.5	21 ± 1	20 ± 1	22 ± 1
t_A (Å)	25 ± 1.5	26 ± 1	25 ± 1	27 ± 1
δ_{SA} (Å)	9 ± 1	10 ± 1	9 ± 1	9 ± 1
ζ_S (Å)	5 ± 1	6 ± 1	9 ± 1	9 ± 1
H (H$_2$O/lipid)	18	16	18	11

5 mN m^{-1} to 27 Å at 40 mN m^{-1} (figure 8, table 5 and electronic supplementary material, figures S9–S11). An increase was also noticed in the Guinier thickness (figure 5), where the slab thickness (t_A) increased from 18 Å at 5 mN m^{-1} to 24 Å at 40 mN m^{-1} (table 2). As with the other DODAB-containing monolayers, the monolayer slab thickness of 24.6 ± 1 Å obtained at a surface pressure of 30 mN m^{-1} using the partial structural analysis (table 5) was comparable with half the thickness of the bilayer of vesicles composed of a 1 : 1 molar ratio of DODAB and DOPE, established to be 48.0 ± 1 Å by Callow *et al.* [47] from small-angle neutron scattering studies.

The area per molecule determined from the Guinier plots agreed with the value determined through partial structure factor analysis, where the area per super-molecule of DODAB : DOPE was found to decrease from 158 Å^2 to 116 Å^2 as the surface pressure increased from 5 mN m^{-1} to 40 mN m^{-1} (table 5). A discrepancy was however noted between the values obtained for area per molecule from the analysis of the SNR datum and those obtained at the same surface pressure from the isotherm (figure 3 and electronic supplementary material, table S1), particularly at surface pressures in the range of 5–30 mN m^{-1}. However, at a surface pressure of 40 mN m^{-1}, there was good agreement between the area per molecules obtained from the SNR analyses (table 5) and those obtained from the isotherm (figure 3). The origin of this discrepancy in the area per molecule obtained at the lower pressures using the two techniques is not known at present but it is worth noting that the best fit to the SNR data obtained for the mixture of DODAB : DOPE (figure 8 and electronic supplementary material, figures S9–S11) deviates slightly at high Q, most probably owing to the two-lipid mixture being imperfectly modelled as a single layer and may, at least in part, explain the discrepancy.

The thickness of the DOPE-containing DODAB monolayer is expected to be thicker than the pure DODAB monolayer because of the greater head group thickness of phosphatidylethanolamine based on its molecular structure. For example, the slab thickness of the DODAB : DOPE monolayer at 40 mN m^{-1} was 27 Å compared with 24 Å for the DODAB-only monolayer at the same surface pressure. The thickness of the solvent layer within the DODAB : DOPE monolayer, ζ_S, increases from 5 to 10 Å as the layer is compressed from 5 to 40 mN m^{-1}, while the solvent separation, δ_{SA}, that is the distance separating the

midpoint of the solvent distribution from the midpoint of the lipid distribution did not change, suggesting that the thickness of the lipid head group region is increasing upon compression of the monolayer owing to one or both of the DODAB or DOPE head groups becoming more vertically oriented.

It is clear from the volume distribution profiles that there is differential wetting of the lipid layer depending on the helper lipid composition, which is especially notable for the DODAB : DOPE monolayer (figure 9). The calculated lipid hydration of up to 18 H$_2$O/lipid molecules for the DODAB : DOPE monolayer (table 5) is rather high and indicates that the DOPE-containing monolayer is more hydrated than the DODAB and DODAB : cholesterol monolayers. Possibly, the DODAB : DOPE layer contains more water because both the amino and phosphate groups of the DOPE are able to establish bonding with water. When in the expanded phase, monolayers of pure phosphatidylethanol-amines (PE) that have the same head group but different lengths of chains and degree of unsaturation were found to have relatively high levels of hydration of 14–19 and 8–10 H$_2$O/PE molecule, by X-ray diffraction and reflection [48] and X-ray diffraction [49], respectively. Water vapour uptake studies have shown that a 1 : 1 molar mixture of egg phosphatidylcholine and egg phosphatidylethanol-amine has an average hydration of 14 H$_2$O molecules compared with just nine H$_2$O molecules per lipid in pure phosphatidylethanolamine films [50], which is consistent with the higher hydration value for DODAB : DOPE monolayers compared with the DODAB mono-layers shown here.

The neutral helper lipids also alter the distribution of charges on the surface of the monolayer, a phenomenon that could affect the DNA-binding capacity. DODAB alone has the greatest charge density (one positive charge per 56 Å^2 at 40 mN m^{-1}) while, at the same surface pressure, upper-limit calculations indicate that the two helper lipids confer a lower charge density on the monolayer, as they are neutral. Assuming that the ionic dissociation of the cationic lipid is unaltered by changes in the monolayer composition, the DODAB : cholesterol monolayer is calculated to have one positive charge per 73 Å^2 and the DODAB : DOPE, discounting the zwitterionic pair of charges, and assuming ideal mixing of the two lipids, has one positive charge per 116 Å^2. This potentially large difference in the spacing of charge is likely to be significant for the ability of these lipids to bind and order DNA, as the distances between adjacent phosphates on the DNA backbone
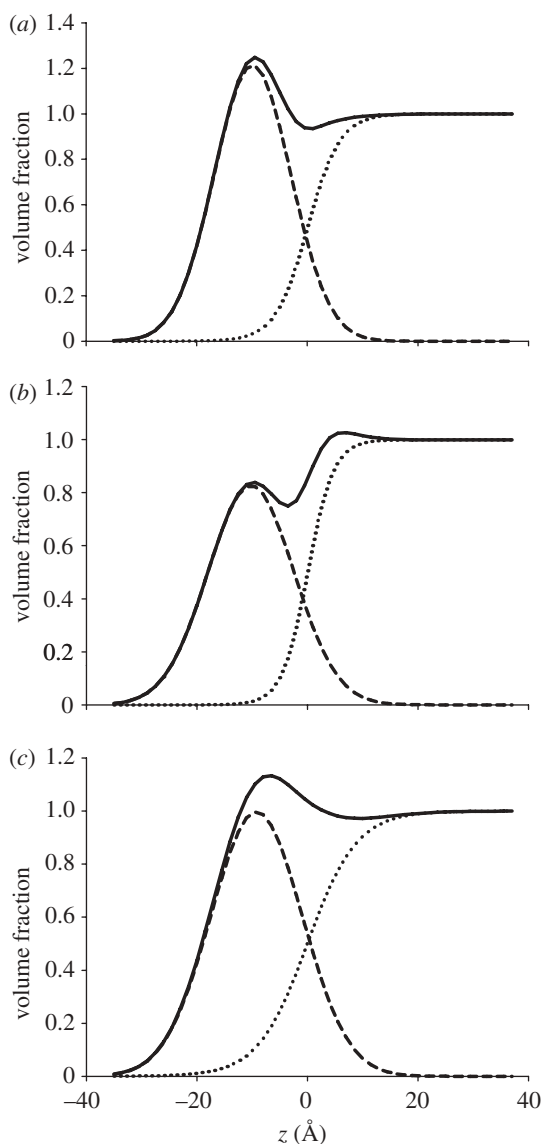
Figure 9. Volume fraction profiles of (*a*) DODAB, (*b*) DODAB : cholesterol and (*c*) DODAB : DOPE monolayers at 40 mN m^{-1}. The profiles of the lipid (dashed line), solvent (dotted line) and the sum of both volume profiles (solid line) are shown.

are fixed. As DNA has two negative charges per base pair and 10 base pairs per turn, a turn of the helix has 20 negative charges over its length of 34 Å [51]. Treating DNA as a cylinder of about 20 Å diameter gives a surface area of 2136 Å per turn, which results in a negative charge per 106 Å^2. On the assumption that our approximations are correct as regards the charge state of DODAB and its uniformity of mixing with the helper lipids, it would appear that mixing of the cationic lipid with helper lipids would help match the charges to the DNA, with DODAB : DOPE matching most closely the charge spacing of DNA. However, this conclusion assumes that DODAB and DOPE are ideally mixed and, as lateral structures are plainly visible in the BAM images obtained for DODAB : DOPE, it is clear that the mixing is not ideal. As a consequence, it is likely that different domains within the monolayer may possess different charge densities resulting in DNA binding more favourably to one over

another. Therefore, DOPE at this mixing ratio is not behaving as a ideal helper lipid and uniformly diluting the DODAB. Further experimental work would be useful in elucidating the domain composition and charge distribution and the effect of the addition of the helper lipid on DNA-binding.

4. CONCLUSIONS

The presence of either of the two neutral helper lipids studied induced significant changes in the structure of monolayers formed by the cationic lipid DODAB, which may have implications for the ability of the lipoplexes formed by these lipids to successfully deliver DNA. Close agreement from the comparison of the thickness of the DODAB monolayers obtained in the present study with half the bilayer thickness of the same lipid systems when in the form of vesicles lends support to the use of monolayer studies to aid in understanding the molecular architecture of the corresponding bilayers. As the lateral surface pressure in the biological membrane is widely considered to be of the order of 30–35 mN m^{-1} (reviewed in [38–40]), it is most pertinent to compare the structure of the various DODAB-containing monolayers at surface pressures between 30 and 40 mN m^{-1}. Analysis of the SNR measurements of the DODAB-containing monolayers showed relatively little difference in the thickness of the various monolayers with the DODAB monolayers exhibiting a Gaussian thickness (i.e. the width of the surfactant distribution, σ), in the range 19–20 Å, while the DODAB : cholesterol and DODAB : DOPE monolayers were very slightly thicker at 20–22 Å. The addition of the helper lipid had very different effects on the phase of the DODAB monolayers at high surface pressures. For example, the DODAB : cholesterol monolayers, like the pure DODAB monolayers, were in a condensed state at 40 mN m^{-1}. Indeed, the presence of cholesterol resulted in a more closely packed structure of the DODAB monolayer at a surface pressure of 40 mN m^{-1} with the area per molecule of the super-molecule (DODAB:cholesterol) having an experimentally obtained area per super-molecule (of 73 Å^2) that was 25 per cent smaller than that obtained by summing the areas per molecule for DODAB and cholesterol, assuming ideal mixing of the two components at the given pressure. The areas per molecule of cholesterol and DODAB at 40 mN m^{-1}, extrapolated from their corresponding Langmuir isotherms, were found to be 39 Å^2 and 58 Å^2, respectively. In contrast, the DODAB film formed in the presence of DOPE was much more expanded (exhibiting an area per super-molecule of 116 Å^2) with only a small condensing effect owing to the DOPE (assuming an area per molecule of DOPE at 40 mN m^{-1} of 72 Å^2 as reported by Rathman & Sun [52] and determined by ourselves).

These differences in the lipid interfacial areas mean that the charge density of the various monolayers could potentially vary very significantly, with the DODAB : DOPE and DODAB monolayers possessing the least and most densely charged layers, respectively. As a helper lipid, cholesterol increases the

spacing of the charges of the monolayer making the charge distribution match that of DNA more closely, assuming that the charge distribution is independent of the film composition. Furthermore, owing to the highly condensed nature of the DODAB and the DODAB : cholesterol monolayers, it might be expected that they would be the monolayers least likely to re-arrange to accommodate a favourable charge interaction with DNA.

Finally, the more heavily hydrated nature of the monolayers containing DOPE compared with the monolayers of DODAB, alone or in combination with cholesterol, at first glance appear to be significant in determining its favourable interaction with DNA. Furthermore, the more expanded nature of the DOPE-containing film may allow it to undergo a re-arrangement to increase binding to DNA. However, the lateral inhomogeneities present in the monolayer indicate that DODAB and DOPE are not ideally miscible on the micron scale as shown by BAM, and that DOPE is not behaving as an ideal helper lipid.

REFERENCES

1 Felgner, P. L., Gadek, T. R., Holm, M., Roman, R., Chan, H. W., Wenz, M., Northrop, J. P., Ringold, G. M. & Danielsen, M. 1987 Lipofection: a highly efficient, lipid-mediated DNA-transfection procedure. *Proc. Natl Acad. Sci. USA* **84**, 7413–7417. (doi:10.1073/pnas.84.21.7413)

2 Lv, H., Zhang, S., Wang, B., Cui, S. & Yan, J. 2006 Toxicity of cationic lipids and cationic polymers in gene delivery. *J. Control. Release* **114**, 100–109. (doi:10.1016/j.jconrel.2006.04.014)

3 Koltover, I. 1998 An inverted hexagonal phase of cationic liposome–DNA complexes related to DNA release and delivery. *Science* **281**, 78–81. (doi:10.1126/science.281.5373.78)

4 Philip, R., Liggitt, D., Philip, M., Dazin, P. & Debs, R. 1993 *In vivo* gene delivery. Efficient transfection of T lymphocytes in adult mice. *J. Biol. Chem.* **268**, 16 087–16 090.

5 Zuhorn, I. S., Kalicharan, R. & Hoekstra, D. 2002 Lipoplex-mediated transfection of mammalian cells occurs through the cholesterol-dependent clathrin-mediated pathway of endocytosis. *J. Biol. Chem.* **277**, 18 021–18 028. (doi:10.1074/jbc.M111257200)

6 Rose, J. K., Buonocore, L. & Whitt, M. A. 1991 A new cationic liposome reagent mediating nearly quantitative transfection of animal cells. *Biotechniques* **10**, 520–525.

7 Dass, C. R., Walker, T. L. & Burton, M. A. 2002 Liposomes containing cationic dimethyl dioctadecyl ammonium bromide: formulation, quality control and lipofection efficiency. *Drug Deliv.* **9**, 11–18. (doi:10.1080/107175402753413136)

8 Engelking, J., Ulbrich, D., Meyer, W. H., Schenk-Meuser, K., Duschner, H. & Menzel, H. 1999 Complexes of an anionic poly(p-phenylene) polyelectrolyte and dioctadecylammonium bromide at the air–water interface. *Mater. Sci. Eng., C* **8–9**, 29–34. (doi:10.1016/S0928-4931(99)00051-X)

9 Vranken, N., Van der Auweraer, M., De Schryver, F. C., Lavoie, H. & Salesse, C. 2002 Formation of highly oriented domains of a thiacarbocyanine dye in a monolayer at the air–water interface. *Langmuir* **18**, 1641–1648. (doi:10.1021/la011164b)

10 da Silva, A. M. G., Romão, R. S., Caro, A. L. & Rodriguez Patino, J. M. R. 2004 Memory effects on the interfacial characteristics of dioctadecyldimethylammonium bromide monolayers at the air–water interface. *J. Colloid Interface Sci.* **270**, 417–425. (doi:10.1016/j.jcis.2003.11.002)

11 Shapovalov, V. & Tronin, A. 1997 Interaction of hydrophobic ions with a langmuir monolayer of dioctadecyldimethylammonium bromide. *Langmuir* **13**, 4870–4876. (doi:10.1021/la962067z)

12 Sun, L., Xu, M., Hou, X. & Wu, L. X. 2004 *In situ* observation of the aggregated morphology and interaction of dialkyldimethylammonium bromide with DNA at air/water interface by Brewster angle microscopy. *Mater. Lett.* **58**, 1466–1470. (doi:10.1016/j.matlet.2003.10.010)

13 Cárdenas, M., Nylander, T., Jönsson, B. & Lindman, B. 2005 The interaction between DNA and cationic lipid films at the air–water interface. *J. Colloid Interface Sci.* **286**, 166–175. (doi:10.1016/j.jcis.2005.01.008)

14 Farhood, H., Serbina, N. & Huang, L. 1995 The role of dioleoyl phosphatidylethanolamine in cationic liposome mediated gene transfer. *Biochim. Biophys. Acta* **1235**, 289–295. (doi:10.1016/0005-2736(95)80016-9)

15 Sternberg, B., Hong, K., Zheng, W. W. & Papahadjopoulos, D. 1998 Ultrastructural characterization of cationic liposome–DNA complexes showing enhanced stability in serum and high transfection activity *in vivo*. *Biochim. Biophys. Acta* **1375**, 23–35. (doi:10.1016/S0005-2736(98)00129-1)

16 Koster, F., Finas, D., Schulz, C., Hauser, C., Diedrich, K. & Felberbaum, R. 2004 Additive effect of steroids and cholesterol on the liposomal transfection of the breast cancer cell line T-47D. *Int. J. Mol. Med.* **14**, 769–772.

17 Faneca, H., Simões, S. & de Lima, M. C. P. 2002 Evaluation of lipid-based reagents to mediate intracellular gene delivery. *Biochim. Biophys. Acta* **1567**, 23–33. (doi:10.1016/S0005-2736(02)00545-X)

18 Barlow, D. J., Ma, G., Webster, J. R. P., Penfold, J. & Lawrence, M. J. 1997 Structure of the monolayer formed at an air–water interface by a novel nonionic (vesicle-forming) surfactant. *Langmuir* **13**, 3800–3806. (doi:10.1021/la970082d)

19 Armen, R., Uitto, O. & Feller, S. 1998 Phospholipid component volumes: determination and application to bilayer structure calculations. *Biophys. J.* **75**, 734–744. (doi:10.1016/S0006-3495(98)77563-0)

20 Léonard, A., Escrive, C., Laguerre, M., Pebay-Peyroula, E., Néri, W., Pott, T., Katsaras, J. & Dufourc, E. J. 2001 Location of cholesterol in DMPC membranes. A comparative study by neutron diffraction and molecular mechanics simulation. *Langmuir* **17**, 2019–2030. (doi:10.1021/la001382p)

21 Penfold, J. & Thomas, R. K. 1990 The application of the specular reflection of neutrons to the study of surfaces and interfaces. *J. Phys. Condensed Matter* **2**, 1369–1412. (doi:10.1088/0953-8984/2/6/001)

22 Crowley, T. L. 1993 A uniform kinematic approximation for neutron reflectivity. *Physica A* **195**, 354–374. (doi:10.1016/0378-4371(93)90163-X)

23 Lu, J. R., Lee, E. M. & Thomas, R. K. 1996 The analysis and interpretation of neutron and X-ray specular reflection. *Acta Crystallogr. A* **52**, 11–41. (doi:10.1107/S0108767395011202)

24 Henderson, J. A., Richards, R. W., Penfold, J., Thomas, R. K. & Lu, J. R. 1993 Organization of poly(ethylene

oxide) monolayers at the air–water interface. *Macromolecules* **26**, 4591–4600. (doi:10.1021/ma00069a027)

25 Goubard, F., Fichet, O., Teyssié, D., Fontaine, D. & Goldmann, M. 2007 Characterization limits of a polymer adsorbed under a monolayer by GIXD measurements. *J. Colloid Interface Sci.* **306**, 82–88. (doi:10.1016/j.jcis.2006.10.016)

26 Gupta, R. K. & Suresh, K. A. 2004 AFM studies on Langmuir–Blodgett films of cholesterol. *Eur. Phys. J. E* **14**, 35–42. (doi:10.1140/epje/i2003-10088-4)

27 Hac-Wydro, K., Wydro, P. & Dynarowicz-Łatka, P. 2005 Interactions between dialkyldimethylammonium bromides (DXDAB) and sterols—a monolayer study. *J. Colloid Interface Sci.* **286**, 504–510. (doi:10.1016/j.jcis.2005.01.094)

28 Kanintronkul, Y., Srikhirin, T., Angsuthanasombat, C. & Kerdcharoen, T. 2005 Insertion behavior of the *Bacillus thuringiensis* Cry4Ba insecticidal protein into lipid monolayers. *Arch. Biochem. Biophys.* **442**, 180–186. (doi:10.1016/j.abb.2005.08.005)

29 Petersen, N. O., Kroon, P. A., Kainoshoa, M. & Chan, S. I. 1975 Thermal phase transitions in deuterated lecithin bilayers. *Chem. Phys. Lipids* **14**, 343–349. (doi:10.1016/0009-3084(75)90071-7)

30 Sunder, S., Cameron, D., Mantsch, H. H. & Bernstein, H. J. 1978 Infrared and laser Raman studies of deuterated model membranes: phase transition in 1,2-perdeuterodipalmitoyl-sn-glycero-3-phosphocholine. *Can. J. Chem.* **56**, 2121–2126. (doi:10.1139/v78-346)

31 Smaby, J. M., Momsen, M. M., Brockman, H. L. & Brown, R. E. 1997 Phosphatidylcholine acyl unsaturation modulates the decrease in interfacial elasticity induced by cholesterol. *Biophys. J.* **73**, 1492–1505. (doi:10.1016/S0006-3495(97)78181-5)

32 Pan, J. J., Tristram-Nagle, S. & Nagle, J. F. 2009 Effect of cholesterol on structural and mechanical properties of membranes depends on lipid chain saturation. *Phys. Rev. E* **80**, 021931. (doi:10.1103/PhysRevE.80.021931)

33 Chiu, S. W., Jakobsson, E., Mashl, R. J. & Scott, H. L. 2002 Cholesterol-induced modifications in lipid bilayers: a simulation study. *Biophys. J.* **83**, 1842–1853. (doi:10.1016/S0006-3495(02)73949-0)

34 Demel, R. A., Van Deenen, L. L. M. & Pethica, B. A. 1967 Monolayer interactions of phospholipids and cholesterol. *Biochim. Biophys. Acta* **135**, 11–19. (doi:10.1016/0005-2736(67)90003-X)

35 Flach, C. R., Mendelsohn, R., Rerek, M. E. & Moore, D. J. 2000 Biophysical studies of model stratum corneum lipid monolayers by infrared reflection–absorption spectroscopy and Brewster angle microscopy. *J. Phys. Chem. B* **104**, 2159–2165. (doi:10.1021/jp9936805)

36 Kahn, J. G., Monroy, F. & Mingotaud, C. 2003 Adsorption of large inorganic polyanions under a charged Langmuir monolayer: an ellipsometric study. *Phys. Chem. Chem. Phys.* **5**, 2648–2652. (doi:10.1039/b212479c)

37 Ruggles, J. L., Baldwin, K. M., Holt, S. A., Foran, G. J. & Gentle, I. R. 2007 Rigid films of an anionic poryphyrin and a dialkyl chain surfactant. *J. Phys. Chem. B* **111**, 5651–5657. (doi:10.1021/jp0677391)

38 Marsh, D. 1996 Lateral pressure in membranes. *Biochim. Biophys. Acta* **1286**, 183–223. (doi:10.1016/S0304-4157(96)00009-3)

39 Demel, R. A., Geurts Van Kessel, W. S. M., Zwaal, F. A., Roelofsen, B. & Van Deenen, L. L. M. 1975 Relation between various phospholipase actions on human red cell membranes and the interfacial phospholipid pressure in monolayers. *Biochim. Biophys. Acta* **406**, 97–107. (doi:10.1016/0005-2736(75)90045-0)

40 Seelig, A. 1987 Local anesthetics and pressure: a comparison of dibucaine binding to lipid monolayers and bilayers. *Biochim. Biophys. Acta* **899**, 196–204. (doi:10.1016/0005-2736(87)90400-7)

41 Callow, P. 2002 Neutron scattering studies of nonionic surfactant vesicles for gene delivery. PhD thesis, King's College London, London, UK.

42 Ma, G., Barlow, D. J., Hollinshead, C. M., Harvey, R. D., Webster, J. R. P. & Lawrence, M. J. 2008 Effects of surface pressure on the structure of the monolayer formed at the air/water interface by a non-ionic surfactant. *J. Colloid Interface Sci.* **317**, 314–325. (doi:10.1016/j.jcis.2007.09.011)

43 Vaknin, D., Kjaer, K., Als-Nielsen, J. & Losche, M. 1991 Structural properties of phosphatidylcholine in a monolayer at the air/water interface: neutron reflection study and reexamination of X-ray reflection measurements. *Biophys. J.* **59**, 1325–1332. (doi:10.1016/S0006-3495(91)82347-5)

44 Jendrasiak, G. L. & Smith, R. L. 2004 The interaction of water with the phospholipid head group and its relationship to the lipid electrical conductivity. *Chem. Phys. Lipids* **131**, 183–195. (doi:10.1016/j.chemphyslip.2004.05.003)

45 Barenholtz, Y. & Gatt, S. 1982 Sphingomyelin: metabolism, chemical synthesis, chemical and physical properties. In *Phospholipids* (eds J. N. Hawthorne & G. B. Ansell), pp. 144. Oxford, UK: Elsevier Biomedical Press.

46 Smondyrev, A. M. & Berkowitz, M. L. 1999 Structure of dipalmitoylphosphatidylcholine/cholesterol bilayer at low and high cholesterol concentrations: molecular dynamics simulation. *Biophys. J.* **77**, 2075–2089. (doi:10.1016/S0006-3495(99)77049-9)

47 Callow, P., Fragneto, G., Cubitt, R., Barlow, D. J. & Lawrence, M. J. 2009 Interaction of cationic lipid/DNA complexes with model membranes as determined by neutron reflectivity. *Langmuir* **25**, 4181–4189. (doi:10.1021/la802847h)

48 Helm, C. A., Tippmann-Krayer, P., Möhwald, H., Als-Nielsen, J. & Kjaer, K. 1991 Phases of phosphatidyl ethanolamine monolayers studied by synchrotron X-ray scattering. *Biophys. J.* **60**, 1457–1476. (doi:10.1016/S0006-3495(91)82182-8)

49 McIntosh, T. J. & Simon, S. 1986 Area per molecule and distribution of water in fully hydrated dilauroylphosphatidylethanolamine bilayers. *Biochemistry* **25**, 4948–4952. (doi:10.1021/bi00365a034)

50 Jendrasiak, G. L. & Mendible, J. C. 1976 Phospholipid head-group orientation: effect on hydration and electrical conductivity. *Biochim. Biophys. Acta* **424**, 149–158. (doi:10.1016/0005-2760(76)90184-3)

51 Mandelkern, M., Elias, J. G., Eden, D. & Crothers, D. M. 1981 The dimensions of DNA in solution. *J. Mol. Biol.* **152**, 153–161. (doi:10.1016/0022-2836(81)90099-1)

52 Rathman, J. F. & Sun, P. 2005 Biocomposite films synthesized at a fluid/fluid interface. *Faraday Discuss.* **129**, 193–203. (doi:10.1039/b410919h)